SLAC – PUB – 4638
June 1988
(T/E)

Search for the Standard Model Higgs Boson at a 1 TeV e^+e^- Collider*

P. R. BURCHAT

Santa Cruz Institute for Particle Physics
University of California, Santa Cruz, California, 95064

D. L. BURKE AND A. PETERSEN

Stanford Linear Accelerator Center
Stanford University, Stanford, California, 94309

ABSTRACT

We have used detailed Monte Carlo simulations to study strategies to search for the Standard Model Higgs boson produced in the reactions $e^+e^- \to Z^0H^0$ and $e^+e^- \to \nu_e\bar{\nu}_eH^0$ at an e^+e^- center-of-mass energy of 1 TeV. We show that it is possible to extract a significant signal from all Standard Model backgrounds if the mass of the Higgs is not near the mass of the $W^\pm$ or Z^0 and is less than 400 (500) GeV when a data sample of 10 (30) fb^{-1} has been collected.

Submitted to *Physical Review D*

---

*Work supported by the Department of Energy, contracts DE-AC03-76SF00515 and DE-AM03-76SF00010.

I. Introduction

The dominant production mechanisms for a neutral Higgs boson at a high-energy e^+e^- collider are $e^+e^- \to Z^0H^0$ and $e^+e^- \to \nu_e\bar{\nu}_eH^0$. The Feynman diagrams for these processes are shown in Fig. 1. For e^+e^- center-of-mass energies $\sqrt{s}$ which are large compared to the particle masses involved, the cross section[1] for $e^+e^- \to Z^0H^0$ decreases as s^{-1} while the cross section[2] for $e^+e^- \to \nu_e\bar{\nu}_eH^0$ increases logarithmically with s. Numerical evaluations of these cross sections at $\sqrt{s} = 1\ TeV$ are given in Table 1 for a range of Higgs masses. The cross section for $e^+e^- \to \nu_e\bar{\nu}_eH^0$ is larger than that for $e^+e^- \to Z^0H^0$ by a factor of about 17 for a Higgs mass of 100 GeV and by a factor of about four for a Higgs mass of 500 GeV.

Because of the larger cross sections for $e^+e^- \to \nu_e\bar{\nu}_eH^0$, we find that for most Higgs masses the largest signal with the highest signal-to-background ratio is from this channel. The one exception is a Higgs with mass near that of the $W^\pm$ or the Z^0. Backgrounds created by the processes $e^+e^- \to e^+\nu_eW^-$ and $e^+e^- \to \nu_e\bar{\nu}_eZ^0$ (Fig. 2b) are kinematically similar to $e^+e^- \to \nu_e\bar{\nu}_eH^0$ and will dominate the signal unless advantage can be taken of the decay properties of the Higgs. Although background to $e^+e^- \to Z^0H^0$ from $e^+e^- \to W^+W^-$ and $e^+e^- \to Z^0Z^0$ (Fig. 2a) will also be large in this mass region, this production mechanism should offer a cleaner signature than the $e^+e^- \to \nu_e\bar{\nu}_eH^0$ process, albeit with a smaller cross section.

We first describe the machine and detector parameters and differential cross sections simulated in the Monte Carlo programs used for this study. We then present our analyses in detail. These analyses naturally divide into two regions according to the mass of the Higgs: a heavy Higgs ($M_H \gtrsim 2M_W$), and the so-called intermediate-mass Higgs ($M_H \lesssim 2M_W$). Finally we comment on methods that may be used to enhance the effectiveness of searches for Higgs particles with masses near those of the W and Z^0.

II. Center-of-Mass Energy Spectrum

The extremely high density to which beam particles must be focused to produce sufficient luminosity to do particle physics at a high-energy e^+e^- collider results in a significant interaction rate between the particles of one beam and the collective electromagnetic fields produced by the particles in the opposite beam. A major consequence of this is that the spectrum of center-of-mass energies at which e^+e^- interactions take place is not at all monochromatic. Radiation of photons during the beam-beam collision ("beamstrahlung") will result in a spectrum of particle interactions that depends in detail on the energy and bunch characteristics of each beam. We have used a spectrum (Fig. 3) that has been calculated[3] for a specific set of beam parameters, but that is typical of most machine designs that have been studied.[4] This calculation includes the effects of multiple radiation and beam-beam disruption for an e^+e^- machine operating at a nominal center-of-mass energy of 1 TeV and a luminosity of $3 \times 10^{33}\, cm^{-2}s^{-1}$. Approximately 30% of the luminosity lies within 2% of the nominal center-of-mass energy squared for the spectrum that we have chosen.

Included in the Monte Carlo simulations are both the effective reduction in center-of-mass energy and the net longitudinal momentum created by the energy loss of each beam. The mean fractional energy loss that particles undergo during the beam-beam collision is denoted by δ and is 0.26 for the spectrum that we have used. We have computed production cross sections (Table 1) by convoluting the luminosity spectrum with each cross section evaluated at the reduced center-of-mass energy of individual e^+e^- pairs. Because of the slow logarithmic dependence of the Higgs production cross section on beam energy for $e^+e^- \to \nu_e\bar{\nu}_e H^0$, beamstrahlung has little effect on the signal rates presented below. The backgrounds are more sensitive to the details of the center-of-mass energy distribution, but we have tried spectra with $\delta = 0.1$, 0.26, and 0.40 and find that the conclusions that we draw from this study are the same for each case.

III. Event and Detector Simulation

We have used Monte Carlo techniques to generate both signal and background events and to simulate the response of the detector. Events containing Higgs particles were generated according to the differential cross sections given in Refs. 1 and 2, and we assume that the Higgs decays according to the Standard Model with three generations of quarks and leptons. The mass of the top quark was assumed to be 40 GeV. The LUND 6.3 model[5] was used to generate $q\bar{q}$ background events and to fragment into hadrons final-state quarks and gluons in all signal and background processes. Our background calculations also include the production of quark and W pairs[6] through the two-photon channel. The two-photon calculation includes a simulation of the distribution of the momentum transverse to the beam line of the gamma-gamma center-of-mass system, but does not include possible[7] enhancement of the photon flux due to the beamstrahlung process. The background process $e^+e^- \rightarrow e^+\nu_e W^-$ was generated with the formulae of Gabrielli.[8]

The properties of a detector that are necessary to successfully carry out a search for a Higgs boson at a high energy e^+e^- collider are easily achievable with current technology. The emphasis in our analysis is on calorimetry and we generally ignore tracking information for hadrons. We also ignore the information which would be supplied by a vertex detector, though we will note at appropriate points which backgrounds can be reduced by isolating heavy quarks in the final state.

To simulate finite detector resolutions and segmentation we modify the generated particle momenta for signal and background processes in the following manner. We assume the azimuthal and polar angles of muons and electrons are well determined by a tracking chamber. The energy of each muon is smeared by a Gaussian distribution with standard deviation

$$\frac{\sigma_E}{E} = 3 \times 10^{-4} E\, GeV^{-1}.$$

This resolution should be achievable, for example, with a drift chamber with radius $1.8\,m$, 72 position measurements each with $200\,\mu m$ resolution, and embedded in a solenoidal magnetic field of 1.0 Tesla. For electrons, we apply the above smearing for low energies and the calorimetric formula

$$\frac{\sigma_E}{E} = \frac{8\%}{\sqrt{E}} GeV^{1/2} + 2\%$$

for high energies, always using the smearing formula which gives the best resolution for a particular energy. We assume that the charges of electrons and muons can be assigned unambiguously.

Photons and charged and neutral hadrons are treated indiscriminately as clusters of calorimetric energy. Tracks within 4° of one another are combined; then the direction of the combined track is smeared by a box function of size $\pm$ 2°. The energies of these tracks are smeared with

$$\frac{\sigma_E}{E} = \frac{50\%}{\sqrt{E}} GeV^{1/2} + 2\%.$$

Finally, to account for possible obstruction of the acceptance of the detector near the beam line by machine components and the hardware needed to support them, we simply ignore tracks within 10° of the beam axis. We assume, however, that the remainder of the detector is completely hermetic, and that the hardware performs well enough to avoid any further loss of sensitivity to the presence of particles in signal or background events.

IV. Heavy Higgs Particles

If the mass of the Higgs exceeds twice the W mass, then the process $e^+e^- \rightarrow \nu_e\bar{\nu}_e H^0$ will be the most favorable source for its discovery. With our assumption that the top quark mass is less than the mass of the W, the Higgs will decay essentially 100% of the time to W^+W^- or Z^0Z^0. We note that if the mass of the top quark is larger than M_W, then the decay $t \rightarrow Wb$ will proceed immediately,

and since the W will carry most of the momentum of the top quark, this case will be very similar to the direct decay of the Higgs to W-pairs.

The signature of the Higgs is a final state of two W or Z^0 bosons which are typically not coplanar due to the transverse momentum generated by the boson propagators present in the production mechanism. (See Fig. 1.) We define acoplanarity as the angle between the two planes that each contain the beam axis and one jet axis. Acoplanarity of zero degrees implies that the two jet axes are pointing in opposite directions in a projection perpendicular to the beam axis. It is very useful to work with momenta in the plane perpendicular to the beam axis in the presence of beamstrahlung, because the beamstrahlung provides a boost for the event along the beam axis but not perpendicular to it. The basic philosophy of our analysis is to search for events in which both W bosons decay to hadrons with little or no energy carried away by neutrinos or other particles that are not observed in the detector. The topology and kinematics of the signal are then used to eliminate backgrounds from QCD and two-photon processes and from $e^+e^- \rightarrow W^+W^-$ events in which a neutrino in the decay chain creates a significant acoplanarity angle.

In all of the analyses described in this paper, we first boost all smeared four-vectors along the z-axis until the vectorial sum of all the z-components of momenta is zero. A thrust analysis is then performed in this boosted frame, and the event is rejected if the angle between the thrust axis and the beam, θ_{thr}, does not satisfy the condition $|\cos\theta_{thr}| < 0.8$. This procedure ensures that the event is well contained in the detector and preferentially rejects processes with differential cross sections which are sharply peaked along the beam axis (for example, $e^+e^- \rightarrow W^+W^-$, $e^+e^- \rightarrow Z^0Z^0$, and $e^+e^- \rightarrow q\bar{q}$).

A cluster analysis is performed with the detected particles in which the cluster-finding algorithm is constrained to divide the event into exactly two clusters. The invariant mass and the vectorial sum of the momenta for each cluster is calculated. We then select events in which the acoplanarity of these cluster

momenta is greater than 10° and the net momentum in the event transverse to the beam line is greater than 50 GeV. These criteria remove two-photon events and $e^+e^- \to W^+W^-$ and $e^+e^- \to q\bar{q}$ events with one or more neutrinos in the final state. To isolate events with W^+W^- in the final state, the mass of the cluster with the smaller mass is required to lie between 66 and 94 GeV while that of the opposite cluster is required to lie between 75 and 110 GeV. We use a W mass of 83 GeV, and the detector simulation indicates that this value should be reconstructed with 13% (FWHM) resolution.

To further reduce backgrounds due to events with large beamstrahlung radiation and/or missing particles, we select events in which the direction of the missing momentum satisfies $|\cos\theta_{miss}| < 0.9$, where θ_{miss} is the angle between the beam axis and the missing momentum in the laboratory frame. We also reject events in which the total visible energy is greater than 600 GeV. This cut removes backgrounds but is extremely efficient for retaining the signal events.

The invariant mass of all particles that are detected in events that pass these requirements is calculated and shown in Fig. 4a and 4b for Higgs masses of 300 and 500 GeV, respectively. The figure gives the number of events that would be detected in a data sample of integrated luminosity 30 fb^{-1}. The estimated background, shown in the figure as a dashed line, is dominated by the $e^+e^- \to W^+W^-$ process, but includes smaller contributions from $e^+e^- \to q\bar{q}$ and two-photon events. The number of signal events surviving the cuts is 125 for a 300 GeV Higgs and 46 for a 500 GeV Higgs; either would easily be observed above the background. Higgs particles with masses above 500 GeV become more difficult to observe because the production cross section decreases with mass and because the width of the Higgs itself increases as M_H^3.

V. Intermediate Mass Higgs Particles

A Higgs boson with mass less than twice M_W will decay to the most massive quark-antiquark pair that is kinematically allowed. With our assumptions this will be either a top or bottom pair depending on the mass of the Higgs. In either

case, the mass of the two jets in the decay will be less than the vector boson masses.

The philosophy of our analysis of the $e^+e^- \to \nu_e\bar{\nu}_e H^0$ reaction with $M_H < 2M_W$ is to search for events that contain two acoplanar jets with masses below that of the W. Some of the selection criteria are very similar to the heavy Higgs analysis. We select events in which $|\cos\theta_{thr}| < 0.7$ and $|\cos\theta_{miss}| < 0.9$ where θ_{thr} and θ_{miss} are defined in the previous section. We reject events if the visible energy is less than $100\,GeV$ or greater than $400\,GeV$. We do a two-cluster analysis and select events in which the acoplanarity of the clusters is greater than 10° and in which the minimum-mass cluster has an invariant mass greater than $1\,GeV$ (to reject leptonic decays of the $W^{\pm}$) and the maximum-mass cluster has an invariant mass less than $50\,GeV$. Finally, events are accepted only if the missing momentum transverse to the beam is greater than $50\,GeV$ and the number of charged particles outside the 10° hole around the beam axis is between 10 and 36.

The reconstructed invariant mass distributions in events with a Higgs of mass $50\,GeV$ and a Higgs of mass $120\,GeV$ are shown in Fig. 5a and 5b, respectively. The probability that an event of the type $e^+e^- \to \nu_e\bar{\nu}_e H^0$ will pass the above selection criteria varies between about 35% and 50% depending on the mass of the Higgs and the decay mode of the Higgs (i.e., the top quark mass).

The background, shown in Fig. 6a, is dominated by the process $e^+e^- \to e^+\nu_e W^-$, but contains contributions from all other processes including the reaction $e^+e^- \to \nu_e\bar{\nu}_e Z^0$ which occurs[9] with a cross section that is about three times the Higgs cross section at $M_H = M_Z$. Both Fig. 5 and Fig. 6 correspond to an integrated luminosity of $30\,fb^{-1}$. The peak bin for the background distribution contains about 25 to 50 times as many events as the peak bin for the signal. The reconstructed mass distribution for background events plus signals from 120 GeV and 150 GeV Higgs particles is shown in Fig. 6b. It should be possible to discover a Higgs with mass greater than $\sim 120\,GeV$ with no further analysis, but

as can be seen in the figure, the visibility of Higgs particles with masses closer to M_W depends critically on the resolution of the detector.

The background from $e^+e^- \to e^+\nu_e W^-$ is very difficult to distinguish from the $e^+e^- \to \nu_e\bar{\nu}_e H^0$ signal because the two processes are kinematically similar. This is demonstrated in Fig. 7 in which the transverse momentum distribution of the $W^\pm$ or H^0 is shown. There are, however, several features of the Higgs decay that might be exploited to enhance the signal with respect to the background. If it is possible to identify heavy quarks in the final state, then the predominance of top or bottom quarks in the Higgs decay will be a powerful signature. We have not addressed this issue further, but it is clear that the ability to place detector components near to the interaction point is extremely desirable.

We also note that the number of detectable charged particles in the final state will be even for the process $e^+e^- \to \nu_e\bar{\nu}_e H^0$, but odd for the process $e^+e^- \to e^+\nu_e W^-$ since the $e^\pm$ in the final state will typically disappear down the beam pipe. If we define the number of detected charged tracks in the event to be the number outside the 10° holes around the beam axis, then we find that approximately 90% of the signal and only 10% of the background events have an even number of charged tracks. The mass distribution for signal plus background is shown in Fig. 8 for events with an even number of detectable tracks. This is the most optimistic improvement in signal-to-background that could be expected unless it is possible to increase the acceptance of the detector. The situation will be less favorable in reality due to tracking inefficiencies created by overlap of particle trajectories, the decays of charged pions and kaons, and asymmetric photon conversions.

We have also investigated the production mechanism $e^+e^- \to Z^0H^0$ which has been previously analysed[10] at lower center-of-mass energies. The cross section for this process is substantial only at lower Higgs masses. (See Table 1.) At large center-of-mass energies, the signature for this mode is two coplanar jets, one of which has the mass of the Z^0. We select events in which $|\cos\theta_{thr}| < 0.8$

since the distribution of the angle of emission of the Z^0 or H^0 with respect to the beam is peaked at 90°. We reject events if the visible energy is less than 400 GeV. We then do a two-cluster analysis and select events in which the acoplanarity of the clusters is less than 5°. To search for a Higgs boson with mass less than the Z^0 mass, we select events in which the mass of the maximum-mass cluster is between 88 and 98 GeV. To search for a Higgs boson with mass greater than the Z^0 mass, we select events in which the mass of the minimum-mass cluster is between 85 and 100 GeV. The probability that an event of the type $e^+e^- \rightarrow Z^0H^0$ will pass the above selection criteria is about 23%, 19% and 29% for a Higgs mass of 50, 100 and 120 GeV, respectively.

The invariant mass distributions for signal events and background events are shown in Figs. 9 and 10, respectively. Each figure represents an integrated luminosity of 30 fb^{-1}. The signals in Fig. 9a and 9b correspond to Higgs masses of 50 and 120 GeV, respectively. Each distribution contains about 300 events. The backgrounds in Fig. 10a and 10b correspond to the selection criteria for a Higgs mass less than the mass of the Z^0 and greater than the mass of the Z^0, respectively. The backgrounds include contributions from $e^+e^- \rightarrow q\bar{q}$, $e^+e^- \rightarrow Z^0Z^0$, and $e^+e^- \rightarrow W^+W^-$ with no one dominant source. It is evident that outside the mass range 75 to 100 GeV the peak signal-to-background ratio is about one, while inside this range the signal is three to four times smaller than the background. As we noted previously, it may be possible to improve the clarity of the signal by identification of the heavy quarks favored in the decay of the Higgs.

VI. Conclusions

The signal for a neutral Higgs boson with mass less than about 50 GeV or between 120 GeV and 500 GeV is clear at an e^+e^- collider with a nominal center-of-mass energy of 1 TeV. The signal is dominated by Higgs production through the W^+W^- fusion process $e^+e^- \rightarrow \nu_e\bar{\nu}_eH^0$.

For a Higgs mass near the mass of the $W^\pm$, there is a large background to

the W^+W^- fusion process from $e^+e^- \rightarrow e^+\nu_e W^-$. For $M_H = M_W$, the signal-to-background ratio is about 1 : 30. However, there are two ways to reduce this background:

- Heavy quark identification — the Higgs will decay almost exclusively to $t\bar{t}$ or $b\bar{b}$ pairs.
- Charged track counting — an efficient charged track counter would provide significant reduction in the background.

The Higgs production mode $e^+e^- \rightarrow Z^0H^0$ does not provide very significant signals at a 1 TeV e^+e^- collider for most Higgs masses. However, this channel provides important cross checks and verifications if the Higgs signal is seen elsewhere, and will provide a visible signal if the Higgs mass is near to the mass of the W or Z^0.

Acknowledgments

This work was part of a larger group effort at SLAC to study the physics opportunities offered by a large high-energy e^+e^- collider. We have benefited from discussions with all members of this group, but in particular with G. Feldman, J. Gunion, and M. Peskin.

Process		Cross Section (fb) Without Beamstrahlung	With Beamstrahlung
$e^+e^- \rightarrow Z^0H^0$	$m_H =$ 50 GeV	12.7	43
	$m_H =$ 100 GeV	12.4	35
	$m_H =$ 150 GeV	12.0	25
	$m_H =$ 300 GeV	9.8	13
	$m_H =$ 500 GeV	5.6	4
$e^+e^- \rightarrow \nu_e\bar{\nu}_eH^0$	$m_H =$ 50 GeV	234	196
	$m_H =$ 100 GeV	216	163
	$m_H =$ 150 GeV	147	124
	$m_H =$ 300 GeV	70	53
	$m_H =$ 500 GeV	23	13
$e^+e^- \rightarrow W^+W^-$		2310	3570
$e^+e^- \rightarrow Z^0Z^0$		127	200
$e^+e^- \rightarrow q\bar{q}$		438	4050
$e^+e^- \rightarrow e^+\nu_eW^-$		9440	8770

REFERENCES

1. J. Gunion, P. Kalyniak, M. Soldate, P. Galison, Phys. Rev. D **34**, 101 (1986).
2. R. Cahn, Nucl. Phys. B **255**, 341 (1985).
3. K. Yokoya, Nucl. Instrum. Methods A251, 1 (1986); P. Chen, SLAC-PUB-4293 (1987).
4. R. B. Palmer, SLAC-PUB 4295 (1987); W. Schnell, Advanced Accelerator Concepts, Madison, WI, AIP Conf. Proc. 156, 12 (1987), and SLAC/AP-61 (1987).
5. T. Sjostrand and M. Bengtsson, Computer Phys. Comm. 43, 367 (1987).
6. M. Katuya, Phys. Lett. 124B, 421 (1987).
7. R Blankenbecler and S. D. Drell, SLAC-PUB-4629 (1988).
8. E. Gabrielli, ROME-550-1987.
9. M. Peskin, private communication.
10. G. Ekspong and K. Hultqvist, USIP Report 82-05 (1982); Proceedings of the Second Mark II Workshop on SLC Physics, SLAC-Report-306 (1986); J. Boucrot *et al.*, CERN-EP/87-40 (1987).

TABLE CAPTIONS

1. Cross sections at an e^+e^- center-of-mass energy of 1 TeV with and without the effects of beamstrahlung.

FIGURE CAPTIONS

1. Feynman diagrams for Higgs production at a high energy e^+e^- collider: (a) $e^+e^- \rightarrow Z^0H^0$, (b) $e^+e^- \rightarrow \nu_e\bar{\nu}_eH^0$.

2. Feynman diagrams for new electroweak background processes that appear in searches for Higgs production at a high energy e^+e^- collider: (a) $e^+e^- \rightarrow W^+W^-$ and $e^+e^- \rightarrow Z^0Z^0$, (b) $e^+e^- \rightarrow e^+\nu_eW^-$ and $e^+e^- \rightarrow \nu_e\bar{\nu}_eZ^0$.

3. Spectrum of the center-of-mass energy used to generate events for this study.

4. Reconstructed mass distribution, after selection criteria, for (a) a Higgs mass of 300 GeV and (b) a Higgs mass of 500 GeV. The Higgs is produced in the process $e^+e^- \rightarrow \nu_e\bar{\nu}_eH^0$. The dotted line corresponds to the expected background.

5. Reconstructed mass distribution, after selection criteria, for (a) a Higgs mass of 50 GeV and (b) a Higgs mass of 120 GeV. The Higgs is produced in the process $e^+e^- \rightarrow \nu_e\bar{\nu}_eH^0$.

6. (a) Reconstructed mass distribution of background events that pass all selection criteria used to search for the Higgs in the reaction $e^+e^- \rightarrow \nu_e\bar{\nu}_eH^0$. This distribution is dominated by the process $e^+e^- \rightarrow e^+\nu_eW^-$ but includes a small contribution from the process $e^+e^- \rightarrow \nu_e\bar{\nu}_eZ^0$. (b) Reconstructed mass distribution for background events plus signals from 120 GeV and 150 GeV Higgs particles.

7. Transverse momentum of (a) the Higgs produced in the reaction $e^+e^- \rightarrow \nu_e\bar{\nu}_eH^0$ and (b) the $W^{\pm}$ produced in the reaction $e^+e^- \rightarrow e^+\nu_eW^-$.

8. Reconstructed mass distribution for background plus Higgs masses of 50 and 120 GeV produced in the reaction $e^+e^- \rightarrow \nu_e\bar{\nu}_e H^0$ for events with an even number of charged tracks outside 10° holes around the beam axis.

9. Reconstructed mass distribution, after selection criteria, for (a) a Higgs mass of 50 GeV and (b) a Higgs mass of 120 GeV. The Higgs is produced in the process $e^+e^- \rightarrow Z^0H^0$.

10. Reconstructed mass distribution of background events that pass all selection criteria used to search for the Higgs in the reaction $e^+e^- \rightarrow Z^0H^0$ for (a) Higgs mass less than the Z^0 mass and (b) Higgs mass greater than the Z^0 mass.

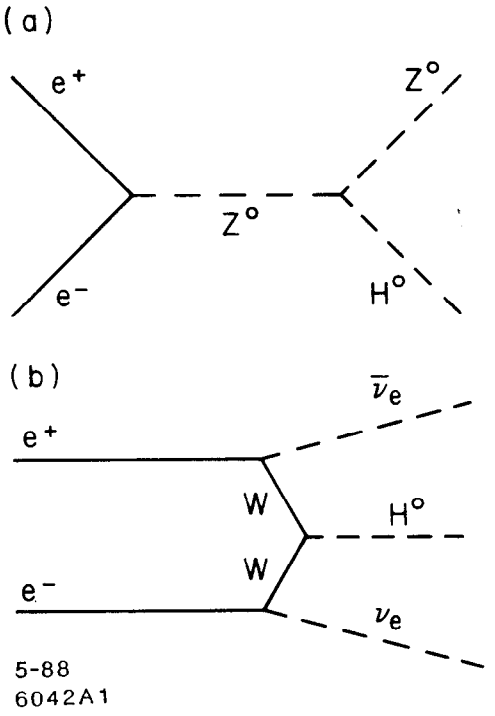

Fig. 1

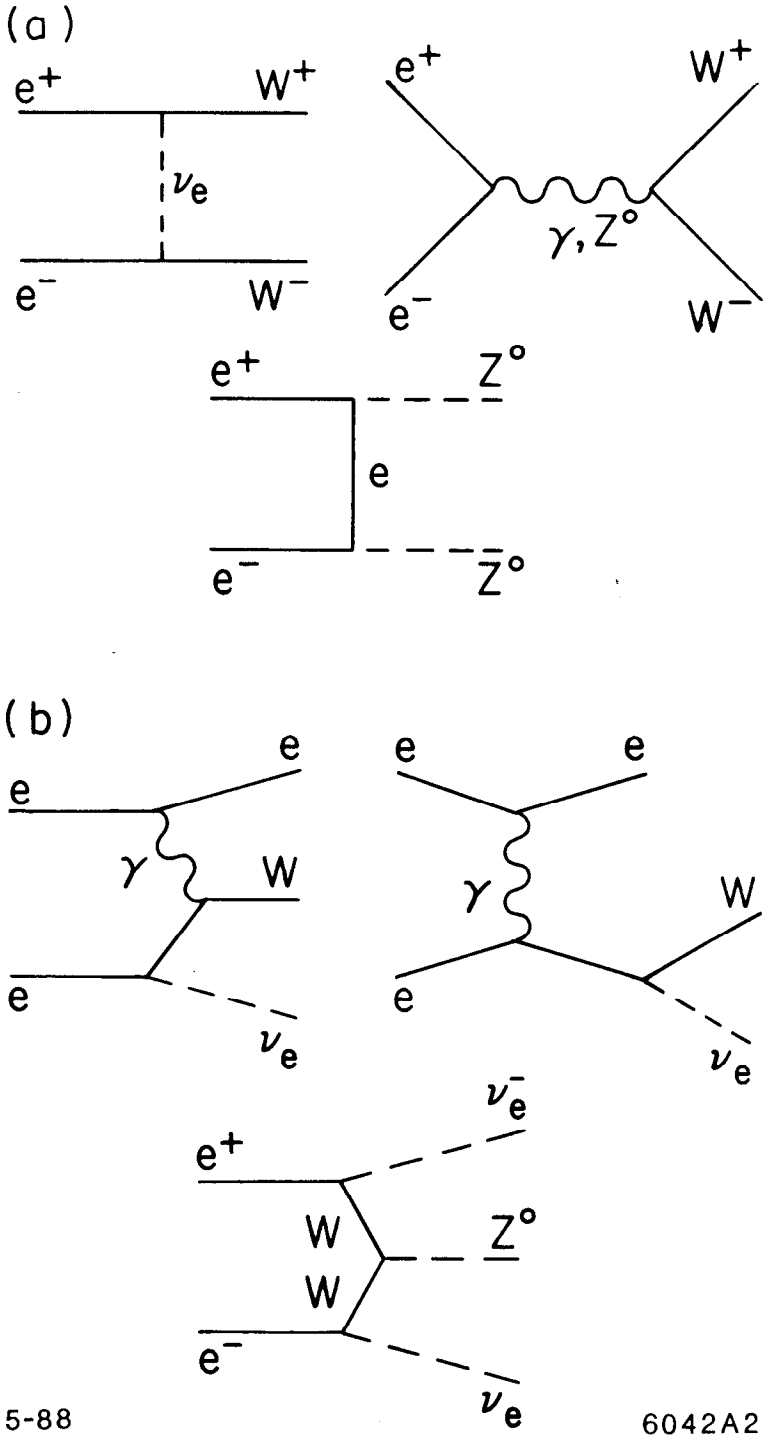
(a)
e+
W+
νe
e−
W−
e+
W+
γ, Z°
e−
W−
e+
Z°
e
e−
Z°
(b)
e
e
γ
W
e
νe
e
e
γ
W
e
νe
ν̄e
e+
W
W
Z°
e−
νe
5-88
6042A2

Fig. 2

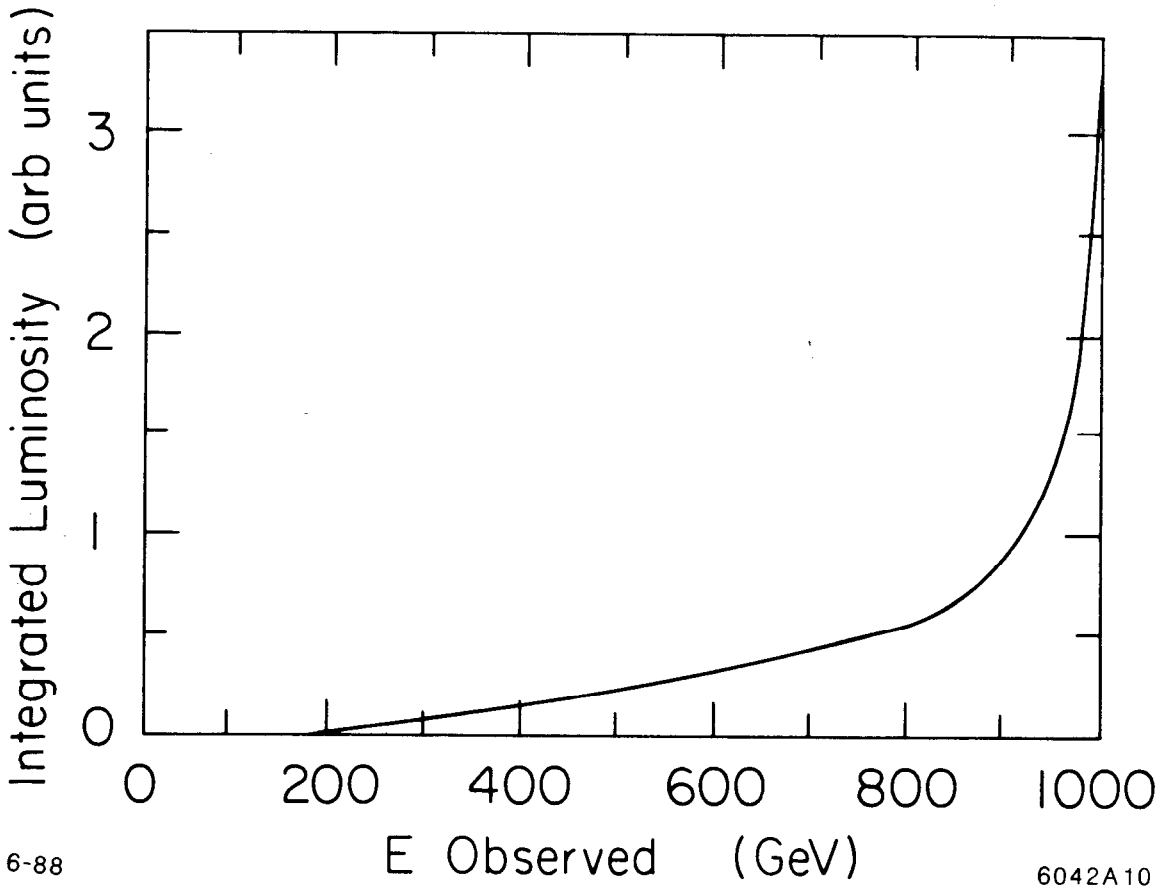
Integrated Luminosity (arb units)
0
1
2
3
0
200
400
600
800
1000
E Observed (GeV)
6-88
6042A10

Fig 3

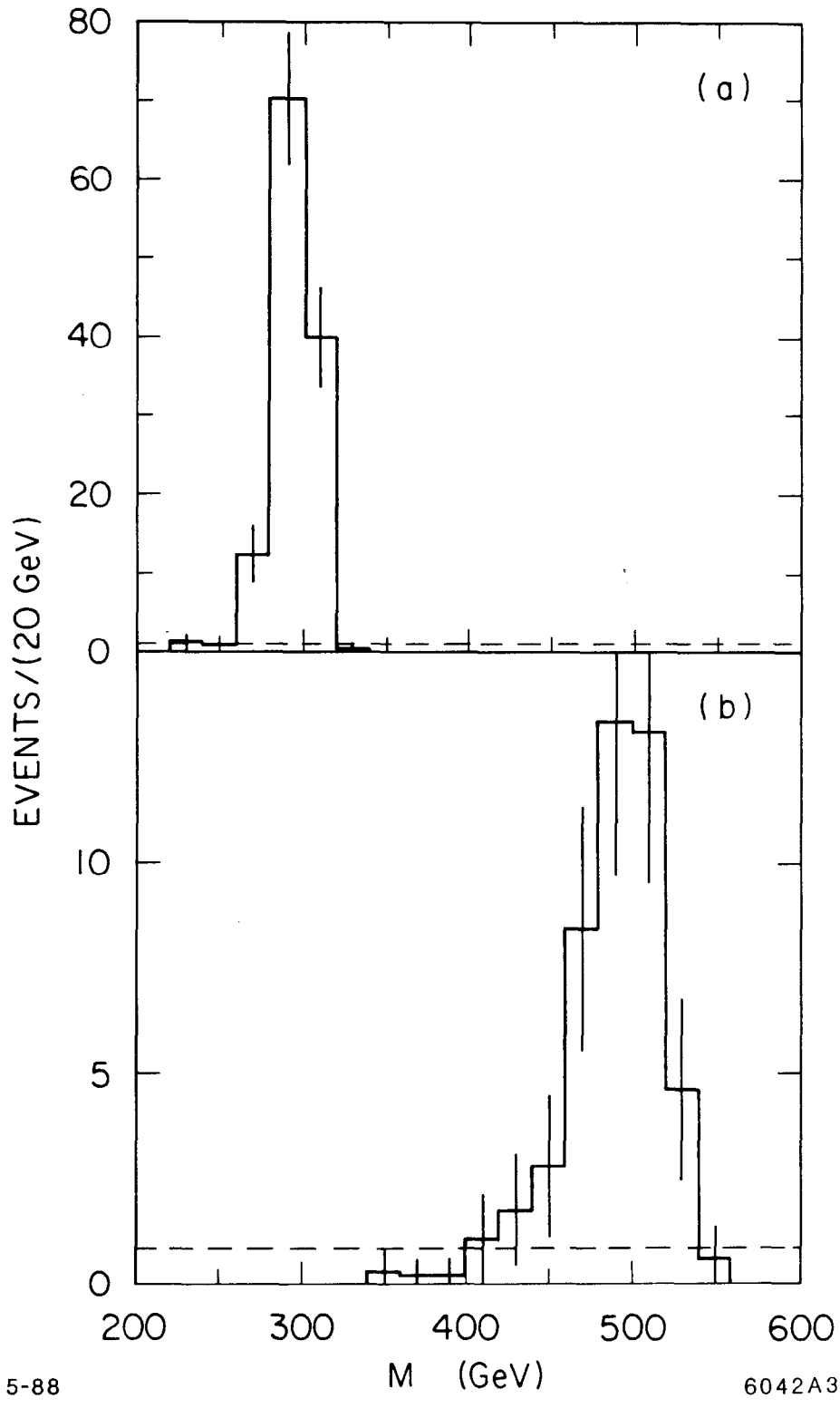
80
60
40
20
0
(a)
(b)
10
5
0
EVENTS/(20 GeV)
200
300
400
500
600
M (GeV)
5-88
6042A3

Fig. 4

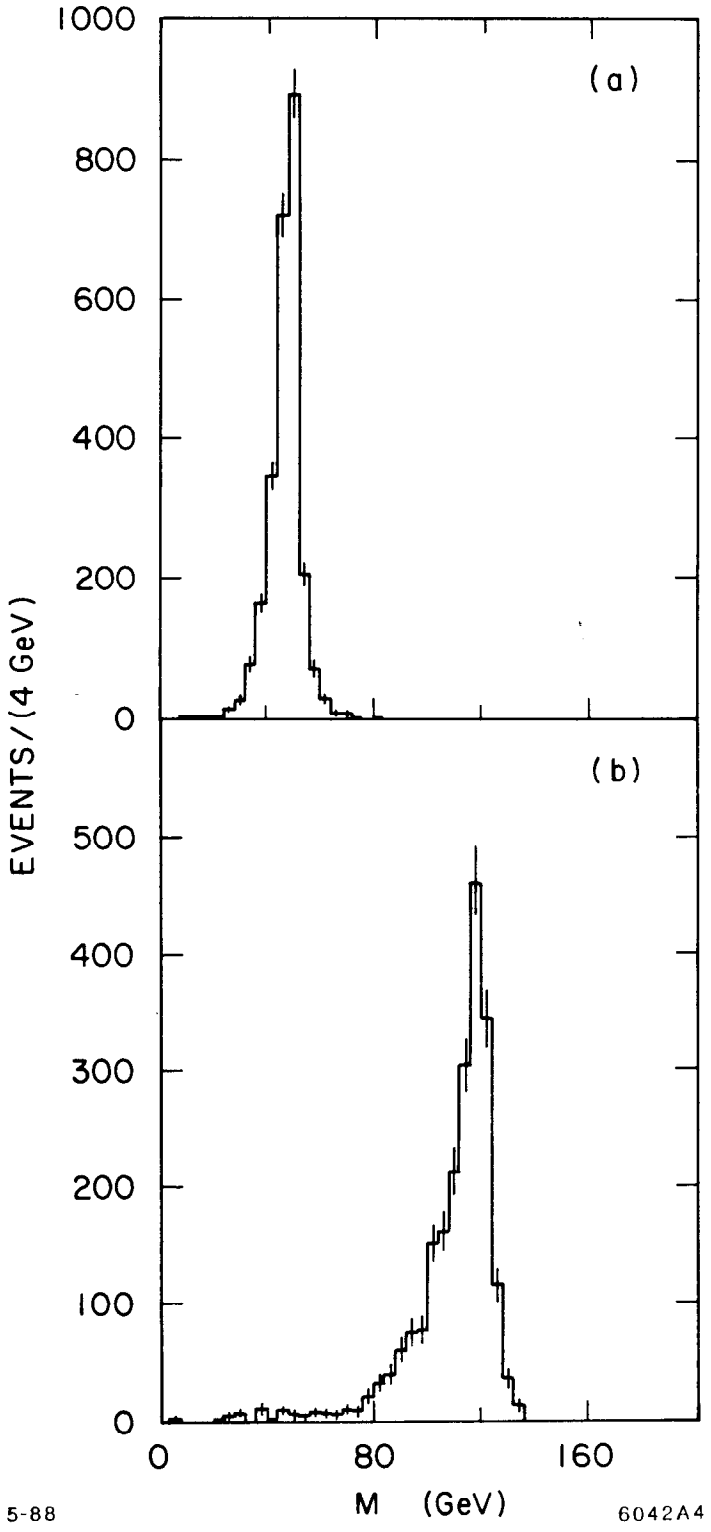
1000
800
600
400
200
0
(a)
EVENTS/(4 GeV)
500
400
300
200
100
0
(b)
0
80
160
M (GeV)
5-88
6042A4

Fig. 5

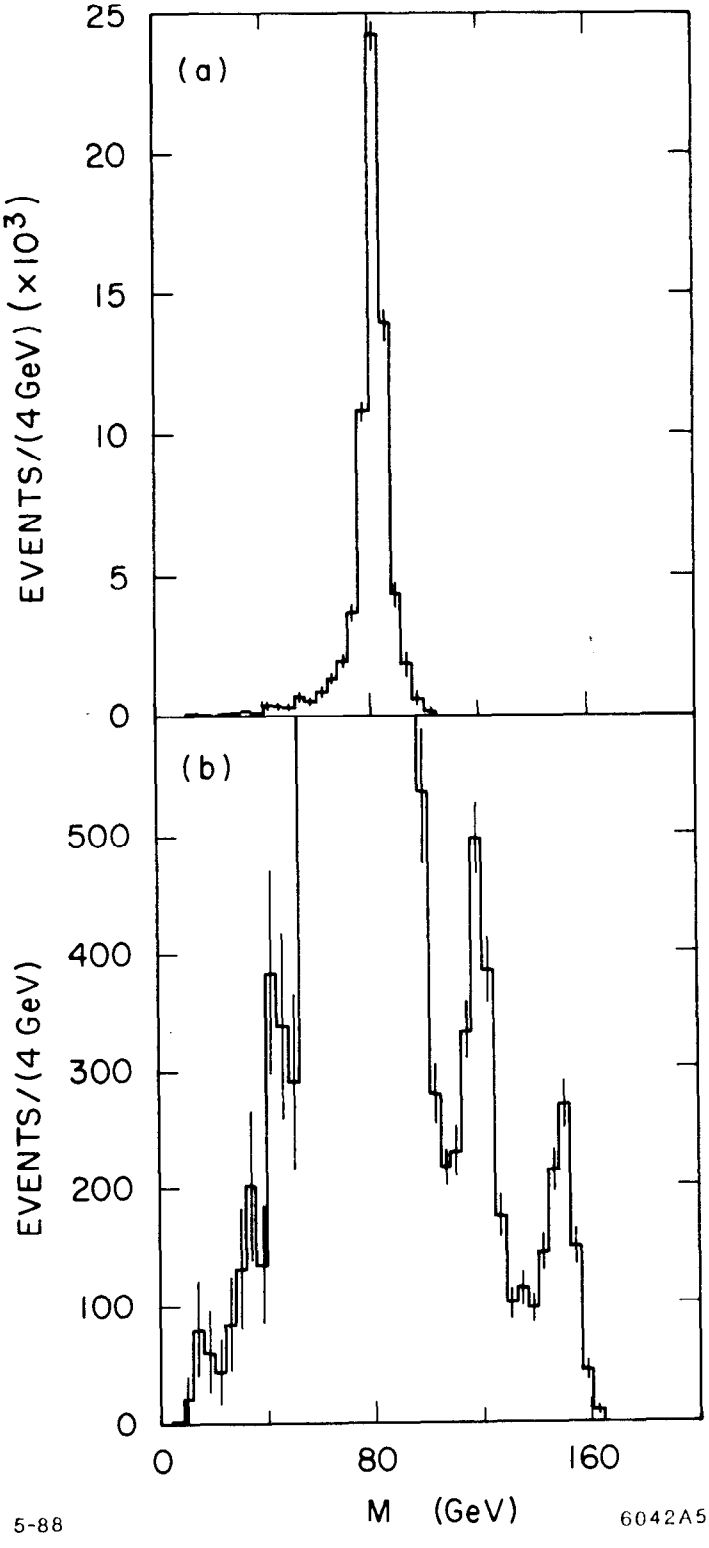
(a)
(b)
EVENTS/(4 GeV) (x10³)
EVENTS/(4 GeV)
25
20
15
10
5
0
500
400
300
200
100
0
80
160
M (GeV)
5-88
6042A5

Fig. 6

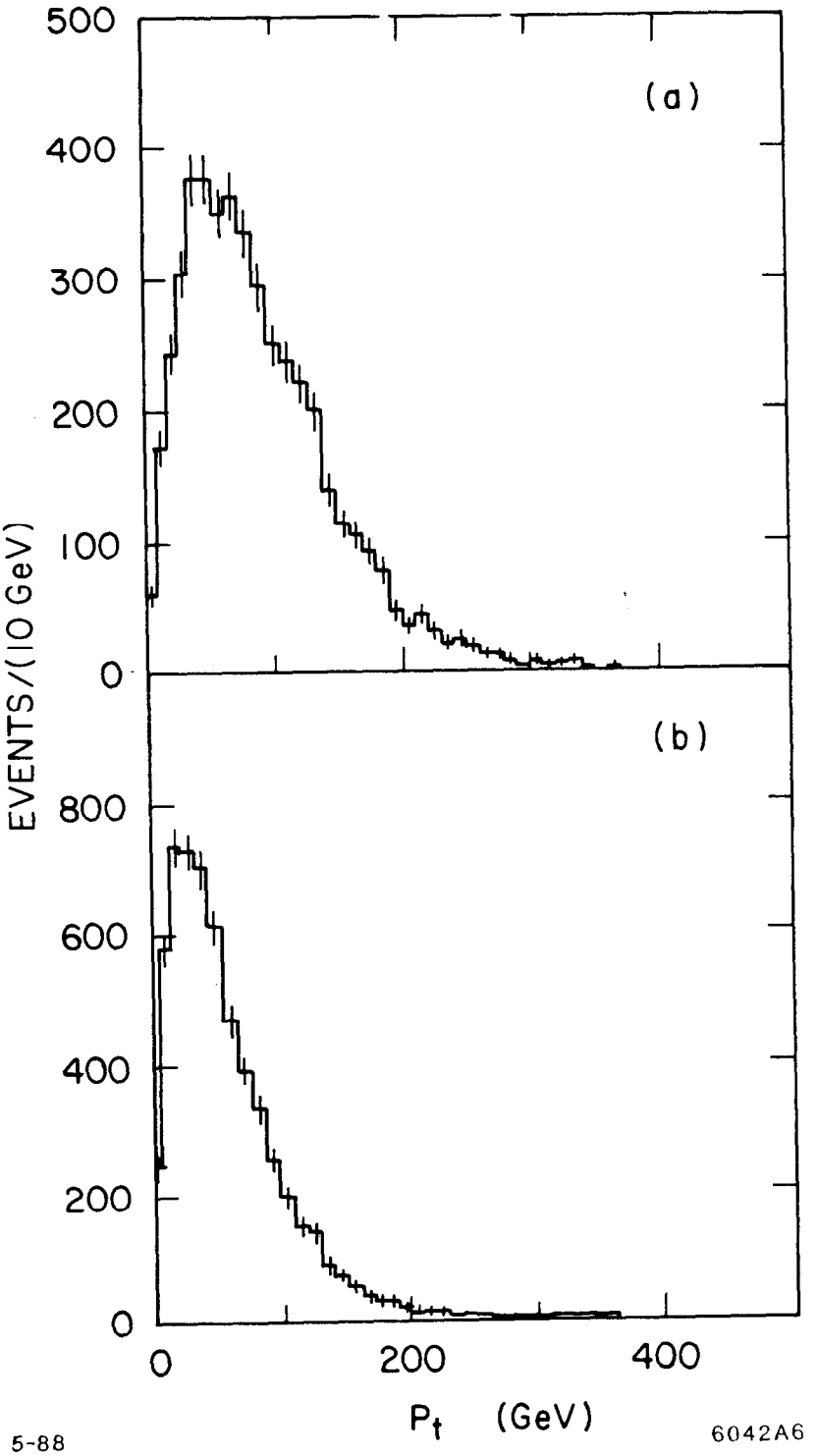
500
400
300
200
100
0
(a)
EVENTS/(10 GeV)
800
600
400
200
0
(b)
0
200
400
P_t (GeV)
5-88
6042A6

Fig. 7

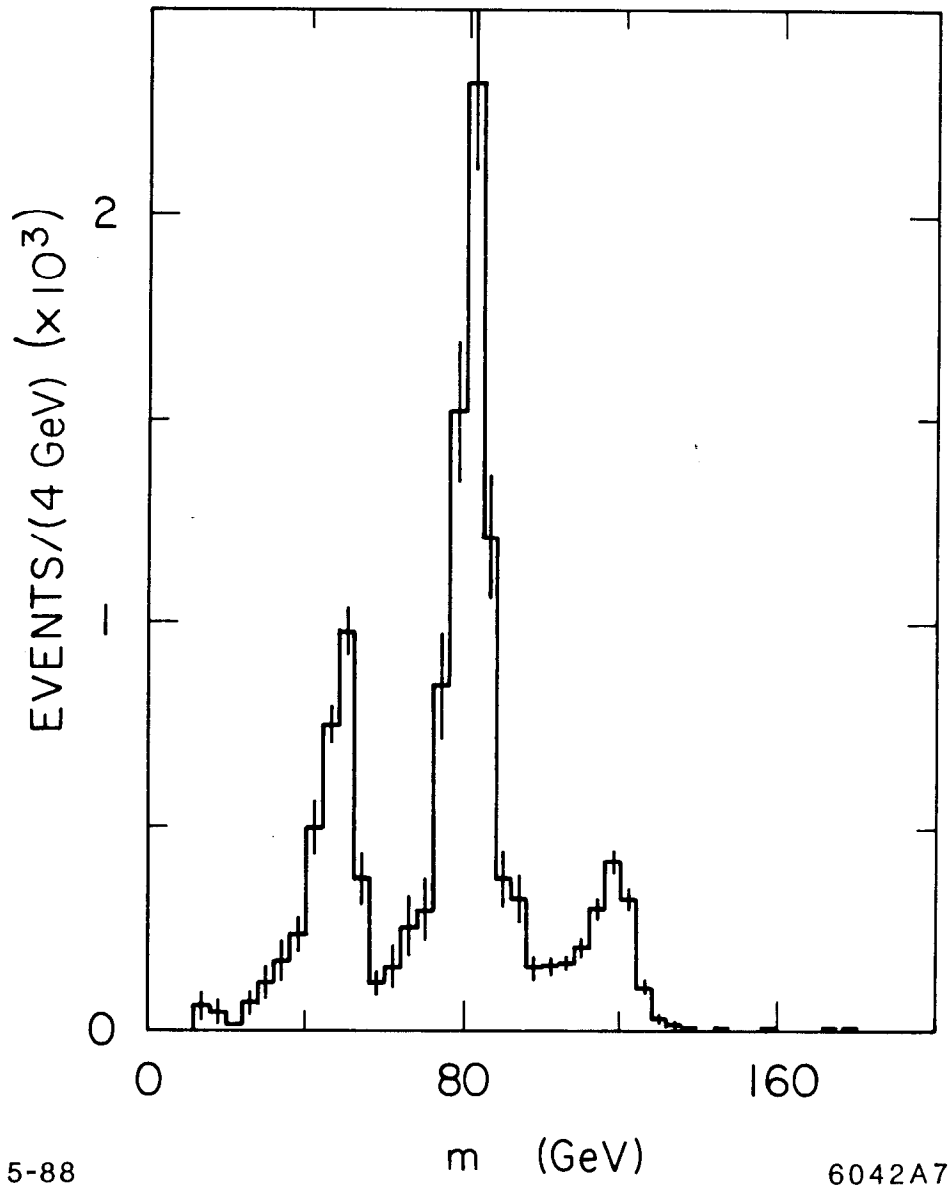

Fig. 8

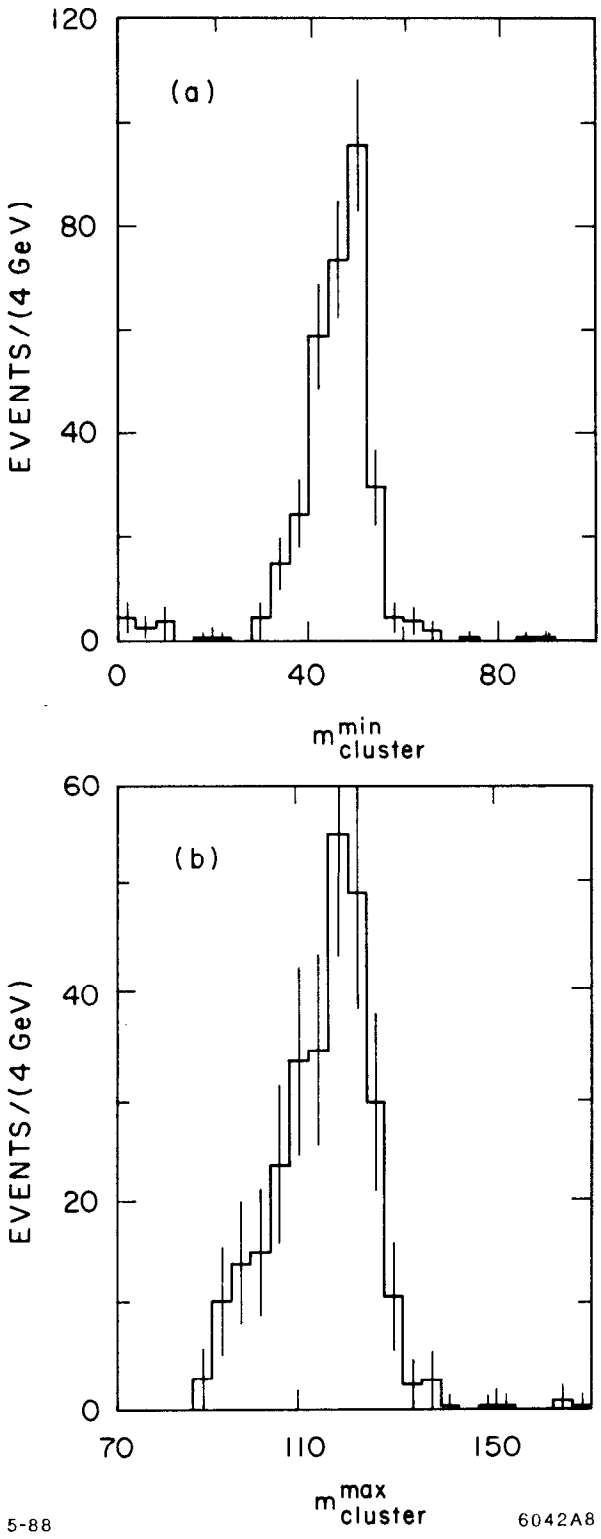
120
80
40
0
EVENTS/(4 GeV)
(a)
0
40
80
$m^{min}_{cluster}$
60
40
20
0
EVENTS/(4 GeV)
(b)
70
110
150
$m^{max}_{cluster}$
5-88
6042A8

Fig. 9

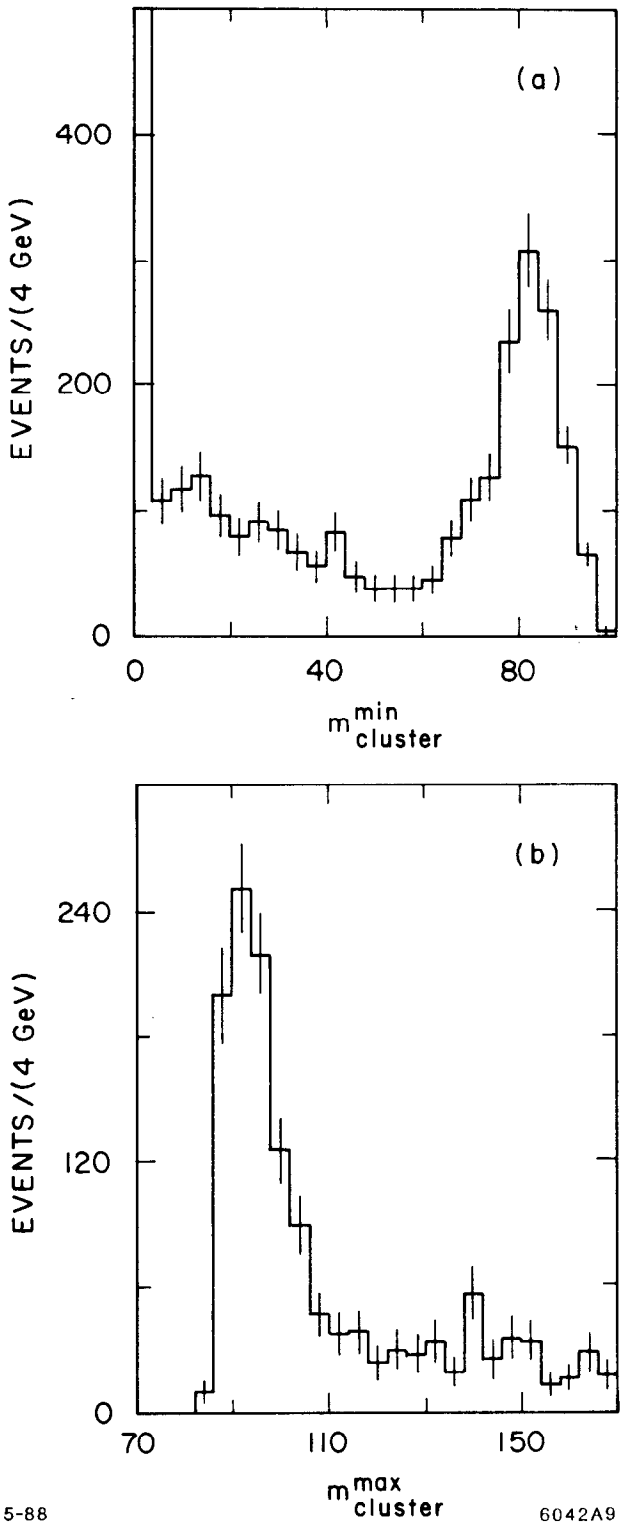
(a)
400
200
0
EVENTS/(4 GeV)
0
40
80
$m^{min}_{cluster}$
(b)
240
120
0
EVENTS/(4 GeV)
70
110
150
$m^{max}_{cluster}$
5-88
6042A9

Fig. 10